

Document downloaded from:

<http://hdl.handle.net/10251/183954>

This paper must be cited as:

Andrade, J.; González Martínez, MC.; Chiralt Boix, MA. (2021). Effect of phenolic acids on the properties of films from Poly (vinyl alcohol) of different molecular characteristics. *Food Packaging and Shelf Life*. 29:1-9. <https://doi.org/10.1016/j.fpsl.2021.100711>



The final publication is available at

<https://doi.org/10.1016/j.fpsl.2021.100711>

Copyright Elsevier

Additional Information

1           **Effect of the processing method on the physicochemical and active**  
2           **properties of poly (vinyl alcohol) films incorporating phenolic acids**

3  
4           Johana Andrade<sup>a</sup>, Chelo González-Martínez<sup>a</sup> and Amparo Chiralt<sup>a</sup>

5  
6           <sup>a</sup> Instituto Universitario de Ingeniería de Alimentos para el Desarrollo, Universitat  
7           Politécnica de València, Camino de Vera s/n, 46022 Valencia, Spain.

8           Corresponding author: joancha@doctor.upv.es; cgonza@tal.upv.es; dchiralt@tal.upv.es

9  
10       **Abstract**

11       Poly (vinyl alcohol) films containing cinnamic acid (C) and ferulic acid (F) at 1 wt  
12       % and 2 wt % were successfully produced by solvent-casting the polymeric  
13       solution and melt blending and compression moulding. The effect of the  
14       processing method and the phenolic acid content on the microstructure,  
15       crystallinity and the optical, thermal, barrier and mechanical properties of partially  
16       hydrolysed poly (vinyl alcohol) based films have been analysed, as well as the  
17       antioxidant and antimicrobial properties of the films. The processing method  
18       influenced the microstructural arrangement of the matrix, leading to differences  
19       in the degree of crystallinity and in the tensile and barrier properties of the films.  
20       The incorporation of phenolic acids, especially ferulic acid, enhanced the barrier  
21       properties of the materials without affecting their thermal stability. The presence  
22       of phenolic acids in the films clearly induced the inhibition of *Listeria innocua*  
23       growth and had a positive antioxidant response, thus suggesting the great  
24       potential of these active materials for food packaging applications.

25  
26       **Keywords**

27       *Cinnamic acid; Ferulic acid; Active films; Cast-films; Thermoprocessed-*  
28       *films; Food packaging.*

29  
30       **1. Introduction**

31       Plastic packaging has become an essential part of the food supply chain  
32       due to its significant role in the preservation of the quality of the food product until  
33       its final consumption (Trabold & Babbitt, 2018). In fact, during the initial stages of  
34       the COVID-19 pandemic, consumer preference for packaged food has

35 skyrocketed, probably due to the increase in online ordering and food delivery,  
36 as packaging is a way of offering consumers reassurance (Kakadellis et al., 2021;  
37 Vanapalli et al., 2021). However, the increasing pressure on the generation of  
38 waste has brought plastic food packaging back into the spotlight amidst growing  
39 public concern about the environmental impact of plastic pollution (Kakadellis et  
40 al., 2021).

41 A great deal of research has successfully reported the development of  
42 biodegradable polymer-based materials that constitute an alternative for the  
43 progressive replacement of synthetic plastics (Brockhaus et al., 2016;  
44 RameshKumar et al., 2020). Poly (vinyl alcohol) (PVA) is a semi-crystalline, water-  
45 soluble and biodegradable polymer that has a high degree of biocompatibility,  
46 while being capable of self-crosslinking due to the high density of hydroxyl groups  
47 located on its side chains (Havstad, 2020). PVA is easily produced by the  
48 saponification of poly (vinyl acetate), a process that allows the molecular weight  
49 and the degree of hydrolysis to be controlled and, consequently, permits the  
50 development of materials with differing degrees of crystallinity, solubility in water  
51 and tensile, barrier and thermal properties (Andrade et al., 2020b). The molecular  
52 characteristics provide PVA with a marked affinity for several active compounds  
53 (Andrade et al., 2020b; Cano et al., 2015), which, when effectively incorporated  
54 into the polymeric matrix, could enable the development of active packaging  
55 materials. Active packaging systems are characterised by interacting dynamically  
56 with the target intrinsic and/or extrinsic factors of the packaged product, whose  
57 action enhances the protective function of the package (Lim, 2015). Additionally,  
58 the partially hydrolysed PVA could be thermo-processed due to the thermo-  
59 protective action of the residual acetate groups in the polymer chain, providing  
60 flexibility in the type of processing used for the development of PVA-based  
61 materials (Andrade et al., 2020b).

62 The processing conditions may result in modifications of the structural  
63 arrangement, especially of the crystalline fraction of semi-crystalline polymers,  
64 which are relevant in view of their effect on the density and the mechanical and  
65 optical performance of the final product, as well as, to a lesser extent, on its  
66 physical aging and long-term stability (Mileva et al., 2018). The processing factors  
67 that are the major influencers on the characteristics of the material are the thermal  
68 history, pressure and flow phenomena. Depending on the polymer structure

69 (molecular weight and polydispersity), the effect of the processing conditions,  
70 such as the increase in cooling rate, can range from simple reductions in  
71 crystallinity to the formation of a completely amorphous structure, nearly always  
72 involving changes in tensile and optical properties. The effects of flow and  
73 pressure, especially important in the injection moulding process, generally modify  
74 nucleation, crystal growth and orientation, with a clear correlation with stiffness  
75 and elongation at break, the effect of which is dominated by the stress applied to  
76 the material (Mileva et al., 2013). Thus, the different processing methods and  
77 their inherent conditions lead to the development of materials with specific final  
78 characteristics, which could determine their application. These changes that films  
79 may undergo could also affect their functionality when incorporating active  
80 agents, especially when using phenolic compounds, such as phenolic acids (PA),  
81 capable of interacting with the hydroxyl and acetate groups of the PVA matrix  
82 (Lan et al., 2019). Of the phenolic acids, cinnamic and ferulic acids are of  
83 increasing potential interest because of their proven antioxidant and antimicrobial  
84 properties (Lima et al., 2019; Mathew & Abraham, 2008; Olszewska et al., 2020).

85 This study aims to evaluate the impact of two types of film processing,  
86 casting and thermo-processing (melt blending and compression moulding), on  
87 the crystallinity and the mechanical and barrier characteristics of partially  
88 hydrolysed PVA films, containing or not cinnamic and ferulic acids as active  
89 agents. To our knowledge, these analyses have not yet been addressed and are  
90 of great interest due to the importance of developing new biodegradable active  
91 materials for safe and sustainable food packaging.

92

## 93 **2. Materials and methods**

### 94 **2.1. Materials**

95 Partially hydrolysed poly (vinyl alcohol) (P) (Mw 13,000–23,000; 87–89%  
96 hydrolysed), glycerol as plasticizer and phenolic acids (PA), cinnamic (C) and  
97 ferulic (F) acid, were purchased from Sigma-Aldrich (Steinheim, Germany).  
98 Magnesium nitrate ( $Mg(NO_3)_2$ ), phosphorus pentoxide ( $P_2O_5$ ) salts, UV-grade  
99 methanol and UV-grade ethanol were supplied by Panreac Química S.A.  
100 (Barcelona, Spain).

101

## 102 **2.2. Preparation of films**

103 Two processing methods, casting (C) of the polymeric aqueous solutions  
104 and melt blending and compression moulding (T), were used to obtain the poly  
105 (vinyl alcohol) films.

106 To cast films, glycerol (10% wt. with respect to the polymer) and phenolic  
107 acids (1% or 2% wt. with respect to the polymer) were added to distilled water  
108 previously heated to 100 °C. After the dissolution of the acids, the polymer (10%  
109 wt.) was incorporated by stirring (1,200 rpm) and heating (100 °C) for 3 h, until  
110 polymer solutions were obtained. Subsequently, all the formulations were  
111 degassed by using a vacuum pump and the solution (equivalent amount to 2 g of  
112 polymer per plate) was subsequently spread evenly onto Teflon plates (150 mm  
113 in diameter). The films were then obtained by drying at controlled temperature  
114 ( $25 \pm 2$  °C) and relative humidity ( $55 \pm 2\%$ ) for 48 h.

115 Thermoprocessed-films were obtained by the compression-moulding of  
116 pellets using a hot plate-press (Model LP20, Labtech Engineering, Thailand).  
117 Pellets were obtained by melt blending the different components by using an  
118 internal mixer (HAAKE™ PolyLab™ QC, Thermo Fisher Scientific, Germany) at  
119 160 °C and 50 rpm, for 10 min. In every case, 10 wt% of glycerol was used with  
120 respect to PVA and the PA was added to the mixture at 1 or 2 g/100 g polymer.  
121 The pellets were cold-milled in a Universal Mill (IKA, model M20, Germany) and  
122 the preconditioned particles (at 53% RH and 25°C) were compression moulded  
123 with a preheating step for 3 min at 160 °C, followed by 3 min thermocompression  
124 at 100 bars. Thereafter, a 3 min cooling cycle was applied. Plasticised films  
125 without PA were used as controls. The different film formulations and the mass  
126 ratio of the respective components are shown in **Table 1**.

127 Cast and thermoprocessed films were conditioned for one week at 25°C and  
128 53% relative humidity (RH) by using  $\text{Mg}(\text{NO}_3)_2$  over-saturated solution before the  
129 characterisation of their functional properties. Films were conditioned at 0% RH,  
130 using  $\text{P}_2\text{O}_5$ , for the analyses of the final PA content in the film, water solubility,  
131 microstructure and thermal behaviour.

132

## 133 **2.3. Characterisation of the active PVA films**

134 2.3.1. Final content of phenolic acids, moisture content and water solubility of the

135 films

136 The final content of the phenolic acids (PA) was determined by solvent  
137 extraction and spectrophotometric quantification. The PA extraction was carried  
138 out by immersing dry samples (25 mg) in 10 mL of a 50% methanol aqueous  
139 solution under stirring at 300 rpm for 48 h. The absorbance ( $A$ ) of the solutions  
140 was measured at wavelengths of 320 nm for ferulic acid (F) and 270 nm for  
141 cinnamic acid (C), using a spectrophotometer (Evolution 201 UV–Vis, Thermo  
142 Fisher Scientific, USA). The PA concentration ( $C_{PA}$ ) was obtained using the  
143 calibration curve of each acid: ferulic acid ( $C_{PA} = (A - 0.005)/0.0852, R^2 =$   
144  $0.995$ ) and cinnamic acid ( $C_{PA} = (A - 0.02)/0.1372, R^2 = 0.992$ ). The  
145 corresponding extracts from the PA-free films were used as backgrounds. The  
146 mass of extracted PA (mg) was compared to the corresponding mass of initially  
147 incorporated PA and the percentage of retention was determined. The  
148 measurements were taken in triplicate.

149 The moisture content of the previously conditioned films (53% RH; 25 °C)  
150 was analysed gravimetrically. Four weighed samples per treatment were dried in  
151 a convection oven (JP Selecta S.A., Barcelona, Spain) at 60 °C for 24 h;  
152 subsequently, these were equilibrated (0% RH; 25 °C) until constant weight.

153 The water solubility was evaluated by a modification of the method  
154 described by Talón, Vargas, Chiralt, & González-Martínez (2019). Dry film  
155 samples (2 cm x 2 cm) inside a mesh, were weighed and placed in a crucible with  
156 10 mL of distilled water for 24 h at 25 °C. The meshes with the remaining film  
157 sample were dried in an oven (J.P. Selecta, S.A., Barcelona, Spain) at 60 °C for  
158 72 h and, subsequently, were transferred to a desiccator with P<sub>2</sub>O<sub>5</sub> until reaching  
159 constant weight. The assay was performed in triplicate and the results were  
160 expressed as g of solubilised film/100 g initial film.

161

### 162 2.3.2. Microstructure and X-ray diffraction analysis

163 The microstructure of the cross-section films was observed using a Field  
164 Emission Scanning Electron Microscope (FESEM) (ZEISS®, model ULTRA 55,  
165 Germany), at an acceleration voltage of 2 kV. Previously, the film samples were  
166 cryofractured by immersion in liquid nitrogen and platinum coated.

167 The degree of crystallinity was analysed through the X-ray diffraction  
168 spectra of the films by means of a D8 Advance X-ray diffractometer (Bruker AXS,  
169 Karlsruhe, Germany). The range  $2\theta$  of evaluation was from  $10^\circ$  to  $50^\circ$ , with a step  
170 size of 0.05, using  $K\alpha$ Cu radiation ( $\lambda$ : 1.542 Å), 40 kV and 40.mA. The diffraction  
171 curves were deconvoluted by using the Lorentz model with the OriginPro 2021  
172 software to define the crystalline and amorphous regions. The ratio of the  
173 crystalline peak area and the total area of the diffractograms defined the degree  
174 of crystallinity of the samples.

175  
176

### 2.3.3. Optical properties

177 The optical properties were determined by measuring the reflectance  
178 spectra of the samples from 400 to 700 nm of wavelength using a  
179 spectrophotometer (CM-3600d Minolta CO., Tokyo, Japan), using both black and  
180 white backgrounds, following the method reported by (Sapper et al., 2018). The  
181 transparency was measured through the internal transmittance ( $T_i$ ), applying the  
182 Kubelka-Munk theory for multiple scattering. CIE  $L^*a^*b^*$  colour coordinates and  
183 chromatic parameters (chroma and hue) were obtained from the reflectance of  
184 an infinitely thick layer of the material by considering D65 illuminant and  $10^\circ$   
185 observer, according to Hutchings (1999). Three measurements were taken from  
186 each film and three films were considered per formulation.

187  
188

### 2.3.4. FTIR characterisation

189 The attenuated total reflection Fourier transformed infrared spectra (ATR-  
190 FTIR) (BRUKE, VERTEX 80, Germany), over the range  $4000-600\text{cm}^{-1}$ , were  
191 analysed for the different samples. These analyses were carried out in triplicate  
192 and at three different locations in each sample.

193  
194

### 2.3.5. Tensile properties and barrier properties

195 The tensile properties of the films were measured using a Universal  
196 Machine (Stable Micro Systems, TA.XT plus, Haslemere, England). Equilibrated  
197 test specimens (25 mm x 100 mm) were mounted in the film extension grips with  
198 an initial separation of 50 mm and stretched at  $50\text{ mm}\cdot\text{min}^{-1}$  until break, following  
199 the standard method ASTM D882-02 (ASTM, 2002). Elastic modulus (EM),

200 tensile strength (TS), and elongation at break point (E) were determined from the  
201 tensile stress ( $\sigma$ ) vs. Hencky strain ( $\epsilon_H$ ) curves. The measurements were taken  
202 in eight samples of each treatment.

203 The water vapour permeability (WVP) was analysed in triplicate following a  
204 standard method, E96/E95M-05 (E. ASTM, 2003). In order to obtain a RH  
205 gradient of 53 to 100%, the samples were placed on Payne permeability cups  
206 (3.5 cm in diameter) (Elcometer SPRL, Hermelle/s Argentau, Belgium) containing  
207 5 mL of distilled water, which were placed inside a desiccator at 25 °C with an  
208 oversaturated  $Mg(NO_3)_2$  solution. The cups were weighed periodically every 1.5  
209 h for 24 h using an analytical balance (0.00001 g). The slopes of the weight loss  
210 vs. time during the steady state period were determined by linear regression to  
211 calculate the water vapour transmission rate (WVTR). WVP was calculated as  
212 described by Cano, Jiménez, Cháfer, González, & Chiralt (2014).

213 The oxygen permeability (OP) in film samples (50 cm<sup>2</sup>) was analysed in  
214 triplicate using an Ox-Tran system (Mocon, Minneapolis, US) at 23 °C and 53%  
215 RH, following a standard method, F1927-07 (F.-07 ASTM, 2004). The OP was  
216 calculated from the oxygen transmission rate multiplied by the average film  
217 thickness and divided by the partial pressure of oxygen. The film thickness was  
218 measured with a digital electronic micrometer (Palmer, COMECTA, Barcelona,  
219 Spain) to the nearest 0.001 mm at six random positions.

220

#### 221 2.3.6. Thermal behaviour

222 The thermal behaviour of the films was assessed by differential scanning  
223 calorimetry (DSC) and thermogravimetric analysis (TGA). For DSC  
224 measurements, the sample was inserted into a hermetically-closed aluminium  
225 pan and placed in a differential scanning calorimeter (DSC 1 stareSystem, Mettler  
226 Toledo, Schwarzenbach, Switzerland), with an empty aluminium pan used as a  
227 reference. The temperature scanning profile was a first heating step from -25 °C  
228 to 250 °C, holding this temperature for 2 min, followed by a cooling to -25 °C,  
229 holding this temperature for 2 min and a second heating step to 250 °C; all of the  
230 scans were run at 10 C/min. For TGA analysis purposes, the samples were  
231 heated in alumina crucibles from 25 °C to 700 °C at 10 °C /min, by using a  
232 thermogravimetric analyser (TGA/SDTA 851e, Mettler Toledo, Schwarzenbach,



233 Switzerland). All of the measurements were taken in triplicate using nitrogen (10  
234 mL/min) as purge gas.

235

### 236 2.3.7. Antioxidant activity

237 The antioxidant capacity of the PVA films was evaluated in terms of the  
238 radical scavenging capacity of the ferulic and cinnamic acids released from the  
239 films into different food simulants. The simulants used were ethanol at 50% (v /  
240 v) in water, as a food simulant of an alcoholic beverage or o/w emulsions, and  
241 ethanol at 95% (v / v), as a simulant of more fatty foods. The DPPH method was  
242 used, as proposed by Aragón-Gutiérrez et al. (2021), with some modifications. A  
243 film sample of each formulation (50 mg) was immersed in 10 mL of the simulant  
244 and kept under constant stirring (300 rpm) at 20 ° C, for 48 h. Afterwards, filtered  
245 aliquots of 500 µL of each extract were mixed with 2 mL of a 0.06 mM DPPH  
246 solution in methanol (Abs 515nm = 0.7 ± 0.2) in a closed cuvette, which was kept  
247 in the dark at room temperature for 60 min. The absorbance was measured at  
248 515 nm by using a spectrophotometer (Evolution 201 UV-Vis, Thermo Fisher  
249 Scientific, USA). The ethanolic extracts of the films without phenolic acids were  
250 used as a control. All of the tests were carried out in triplicate and the DPPH  
251 radical scavenging activity was expressed as % according to Equation (1)

252

$$253 \text{ Scavenging of DPPH (\%)} = \frac{A_C - A_S}{A_C} \times 100 \quad (1)$$

254

255 Where  $A_C$  and  $A_S$  are the absorbance of the black control and the tested  
256 sample, respectively.

257

### 258 2.3.8. Antimicrobial activity

259 The antimicrobial activity of the active PVA films was evaluated by means  
260 of the agar diffusion method with slight modifications (Brito et al., 2021) against  
261 *Escherichia coli* (CECT 515), Gram (+), and *Listeria innocua* (CECT 910), Gram  
262 (-), obtained from Spanish Type Culture Collection (CECT, Burjassot, Spain).  
263 The bacterial strains, stored under protective conditions (glycerol 30%) at -25 °C,  
264 were regenerated as described by Valencia-Sullca et al. (2016), by incubating

265 them at 37 °C for 24 h in tryptic soy broth (TSB) (Scharlab, S.L., Barcelona, Spain)  
266 and harvested in their exponential growth phase. The active cultures were  
267 properly diluted in tryptone phosphate water (Sharlab S.A., Barcelona, Spain) to  
268 obtain a target inoculum of 10<sup>5</sup> colony-forming units (CFU)/ml.

269 The films were cut into discs (10 mm in diameter) and sterilised under UV  
270 light before the antimicrobial tests. Circular samples were carefully placed on the  
271 inoculated plates with 1 mL inoculum. Culture media in the plates were 10 mL of  
272 violet red bile agar (VRBA) (Scharlab, S.L., Barcelona, Spain) for *E. coli* and  
273 palcam agar base (PAB) (Scharlab, S.L., Barcelona, Spain), enriched with  
274 palcam selective supplement, for *L. innocua* (Scharlab, S.L., Barcelona, Spain).  
275 The petri dishes were then incubated at 10 °C for 7 days in the incubation  
276 chamber. The plates were examined to measure the halo of inhibition of the film  
277 discs. Five replicates were carried out for each film.

278

### 279 **3. Results and Discussion**

#### 280 **3.1. Phenolic acid and moisture content in the films, and their water** 281 **solubility**

282 The final phenolic acid content (PA) in the films is shown in Table 1. In every  
283 case, the remaining amount of PA was lower than that initially incorporated. The  
284 retention percentage ranged between 90-77% for cast films and 72-20% for  
285 thermoprocessed samples. The losses were higher for films containing ferulic  
286 acid, especially in thermoprocessed films. Therefore, the losses of active  
287 compound depended on the type of phenolic acid and the type of film processing.  
288 The combined effect of high temperature, shearing stress and pressure  
289 conditions given in thermo-processing provoked significantly greater reductions  
290 in the final PA concentration of the thermoprocessed films than those obtained in  
291 cast-films. Cinnamic acid (C) has greater thermal stability than ferulic acid (F),  
292 which could explain its greater retention in the films. However, the onset  
293 temperature of degradation (230 °C for cinnamic acid and 210 °C for ferulic acid)  
294 of both acids is higher than that applied during melt blending (160 °C) or  
295 compression moulding. Therefore, the losses could not be principally attributed  
296 to compound degradation brought about by thermal effect, but rather to the fact  
297 that their antioxidant nature causes oxidative degradation, under the process

conditions. In fact, the UV spectra of the compounds extracted from films for their spectrophotometric analyses revealed changes in the UV spectral pattern with respect to the standard compounds in the case of ferulic acid (**Annex 1**) that had a greater antioxidant capacity (Li et al., 2021). These changes must be associated with the presence of modified molecular structures produced by the partial oxidation of the active. (Aragón-Gutiérrez et al., 2021) also reported 30% losses of ferulic acid in EVOH films obtained by melt extrusion at 190 °C, but with a shorter residence time (3 min). Oxidative processes will also be affected by the exposure time of the material to the processing conditions. A reduction of 40% in the case of ferulic acid and 5% in that of cinnamic acid were also observed for starch films obtained by thermo-processing at 130 °C (Ordoñez et al., 2021).

**Table 1.** Nominal mass fraction of the film components and final content of cinnamic (C) or ferulic (F) acids at 1 or 2%. The ratio between the determined final content and the incorporated amount of phenolic acid (% retention), the equilibrium moisture content and the water solubility (% of solubilised solids) were also shown for films obtained by casting (C subscript) and thermo-processing (T subscript). Mean values and standard deviation in brackets.

Sample	$X_{PVA}$	$X_{GLy}$	$X_{PA}$	Final PA content in the films		Equilibrium Moisture Content (%)	Water solubility (%)
				mg PA/g PVA	Retention (%)		
P <sub>C</sub>	0.91	0.09	0	-	-	6.0 (0.1) <sup>d,2</sup>	80 (6) <sup>a,2</sup>
PC1 <sub>C</sub>	0.9	0.09	0.01	9.1 (0.16)	90.8 (0.6) <sup>c,2</sup>	5.7 (0.2) <sup>bc,2</sup>	75 (3) <sup>a,1</sup>
PC2 <sub>C</sub>	0.89	0.09	0.02	17.2 (0.8)	86.0 (4.0) <sup>b,2</sup>	5.5 (0.2) <sup>ab,2</sup>	82 (5) <sup>ab,1</sup>
PF1 <sub>C</sub>	0.9	0.09	0.01	7.8 (0.3)	78.0 (3.0) <sup>a,2</sup>	5.5 (0.1) <sup>a,1</sup>	74 (1) <sup>a,1</sup>
PF2 <sub>C</sub>	0.89	0.09	0.02	15.4 (0.1)	77.0 (0.3) <sup>a,2</sup>	5.9 (0.1) <sup>cd,2</sup>	90 (1) <sup>b,1</sup>
P <sub>T</sub>	0.91	0.09	0	-	-	5.8 (0.5) <sup>b,1</sup>	68 (3) <sup>a,1</sup>
PC1 <sub>T</sub>	0.9	0.09	0.01	8.32 (0,03)	83.0 (0,3) <sup>d,1</sup>	5.3 (0,0) <sup>a,1</sup>	72 (3) <sup>ab,1</sup>
PC2 <sub>T</sub>	0.89	0.09	0.02	14,4 (0,5)	72.0 (3.0) <sup>c,1</sup>	5.2 (0.1) <sup>a,1</sup>	85 (1) <sup>c,1</sup>
PF1 <sub>T</sub>	0.9	0.09	0.01	1,99 (0,04)	19.9 (0.4) <sup>a,1</sup>	5.4 (0.0) <sup>a,1</sup>	83 (7) <sup>c,1</sup>
PF2 <sub>T</sub>	0.89	0.09	0.02	5,5 (0,2)	27.0 (1.0) <sup>b,1</sup>	5.3 (0.0) <sup>a,1</sup>	81 (9) <sup>bc,1</sup>

Different superscript letters indicate significant differences between formulations within the same processing method, while different numbers indicate significant differences between formulations with equivalent mass fractions but processed by different methods ( $p < 0.05$ ).

\*(Single 2-columns)

320

321 The equilibrium moisture of PVA films was affected by the PA incorporation,  
322 which reduced the water sorption capacity in both cast and thermoprocessed  
323 films. This may be due to the formation of hydrogen bonds between the OH  
324 groups of the polymer chains and the carboxyl or phenolic groups of PA, which  
325 should reduce the number of active points of the PVA chains for bonding water  
326 molecules (Hernández-García et al., 2021). In general, thermoprocessed films  
327 exhibited slightly lower values of moisture content than cast films, which could be  
328 attributed to the different chain rearrangement obtained in each case and the  
329 different interchain bond established, which can modify the active points of the  
330 matrix to bond water molecules.

331 As regards the water solubility values, films without phenolic acids obtained  
332 by casting (Pc) presented significantly higher solubility values (80%) than  
333 thermoprocessed films (Pt) (68%). However, the incorporation of phenolic acids  
334 promoted changes in the water solubility of the films, but these were only  
335 significant in thermoprocessed films. This could be due to the partial hydrolysis  
336 induced in the polymer chains by phenolic acids at the high processing  
337 temperature.

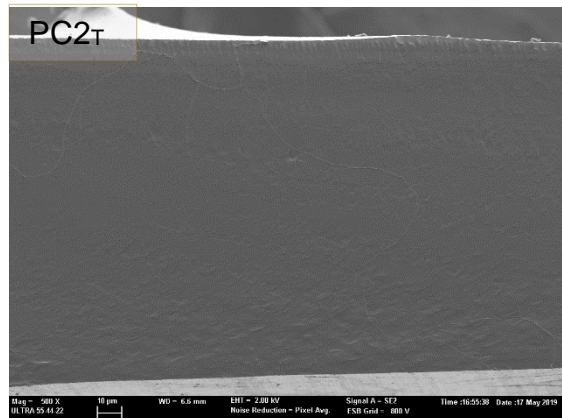
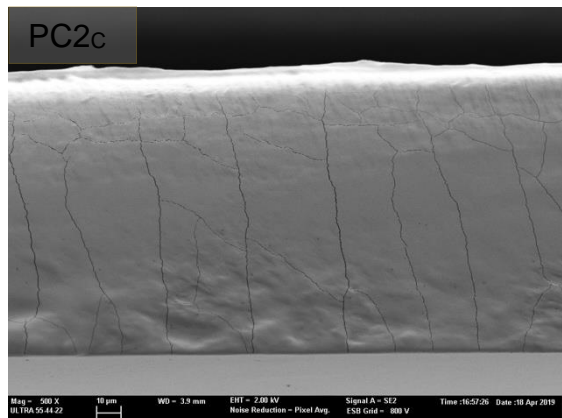
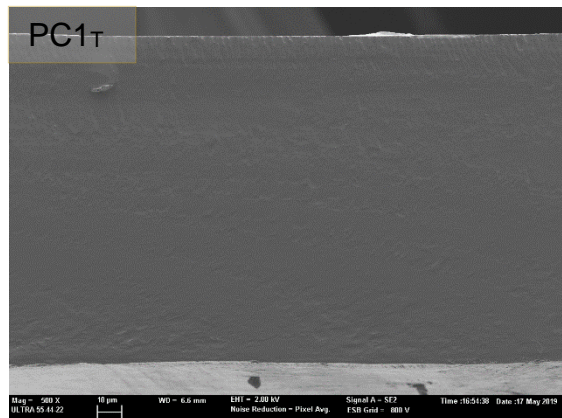
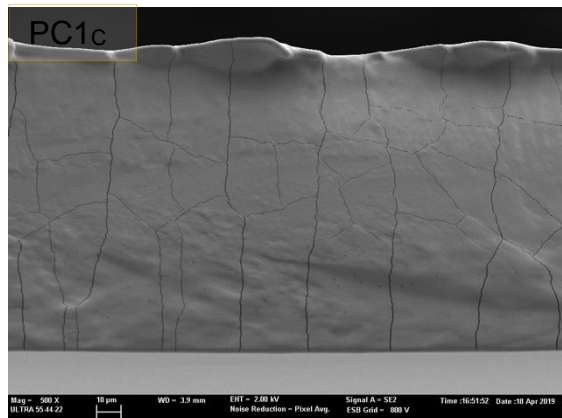
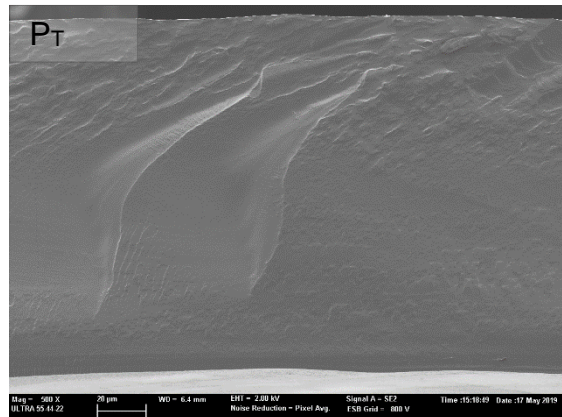
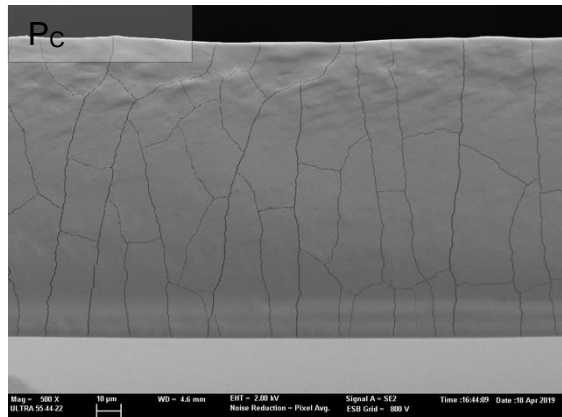
338

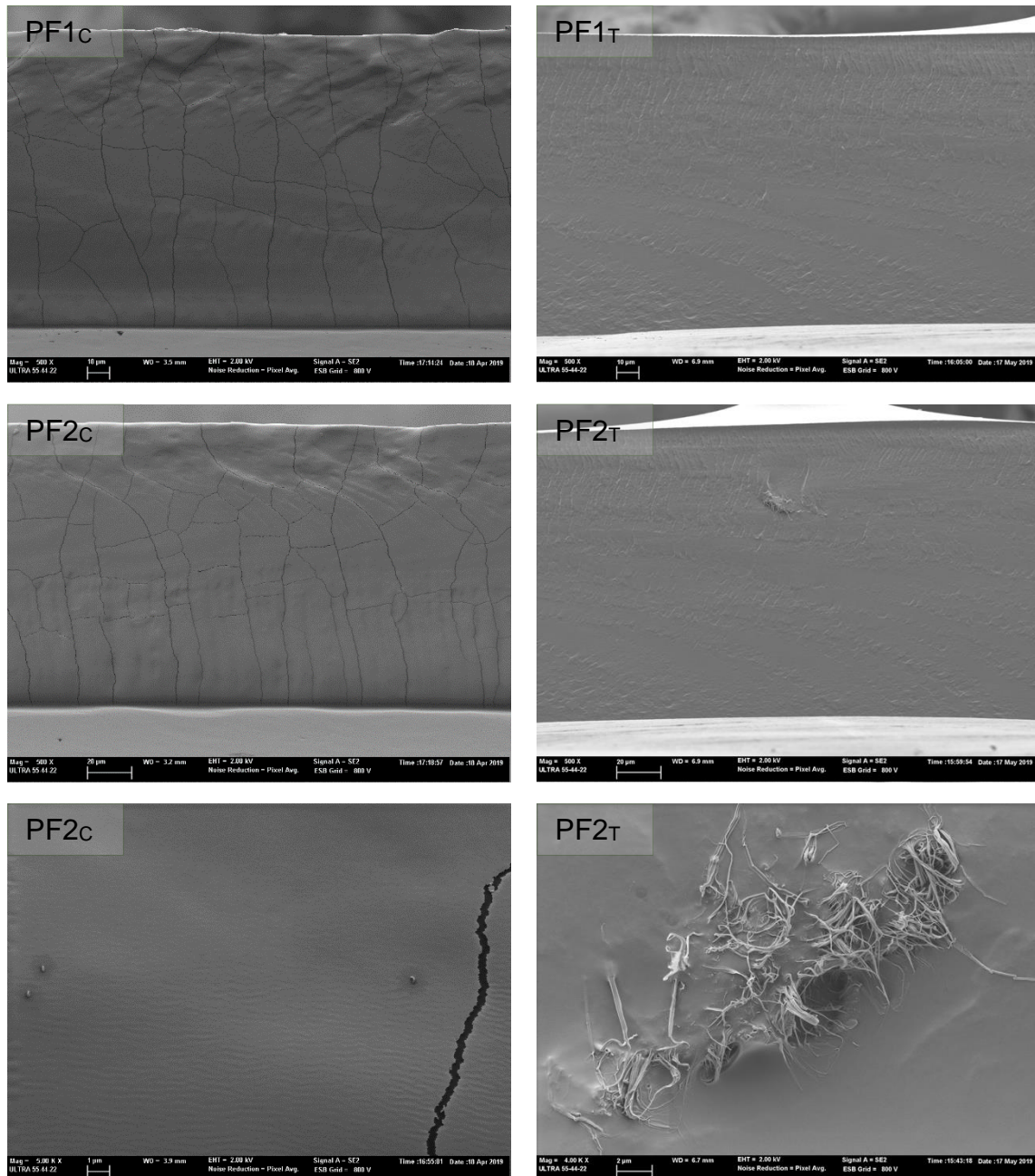
### 339 **3.2. Microstructure and crystallinity of the films.**

340 The PVA films obtained both by casting and by thermo-processing presented a  
341 smooth and homogeneous appearance, as observed in **Figure 1**. The  
342 incorporation of PA did not generate marked modifications in the structure of the  
343 film matrix, which suggests that the acids presented a chemical affinity with the  
344 polymeric matrix. Nevertheless, at higher magnification, different structural  
345 features could be observed for films with phenolic acids, as shown in **Figure 1**  
346 for ferulic acid. Thermoprocessed films exhibited some domains with a rubbery  
347 cryofracture (image of higher magnification in Figure 1), which suggests the  
348 presence of highly plasticised regions in the film. Likewise, few dispersed acid  
349 particles of approximately 200 nm were observed in all the cast films (image of  
350 higher magnification in Figure 1). This could be attributed to the local  
351 aggregation/precipitation of PA molecules during film drying, caused by  
352 oversaturation in the polymeric solution in line with water loss. This local  
353 oversaturation of acids at high temperatures (thermoprocessing) could promote

354 partial hydrolyses at some points of the PVA matrix, thus provoking local  
355 plasticised regions with the observed rubbery fracture.

356





357 **Figure 1.** Field Emission Scanning Electron Microscope (FESEM) micrographs  
 358 of the cross-section of the PVA (P) films with cinnamic (C) or ferulic (F) acid (1 or  
 359 2 g/100 g PVA) obtained by casting (C) or thermo-processing (T) (500X).  
 360 Micrographs at higher magnification (4k-5k X) were included for films with 2%  
 361 ferulic acid.

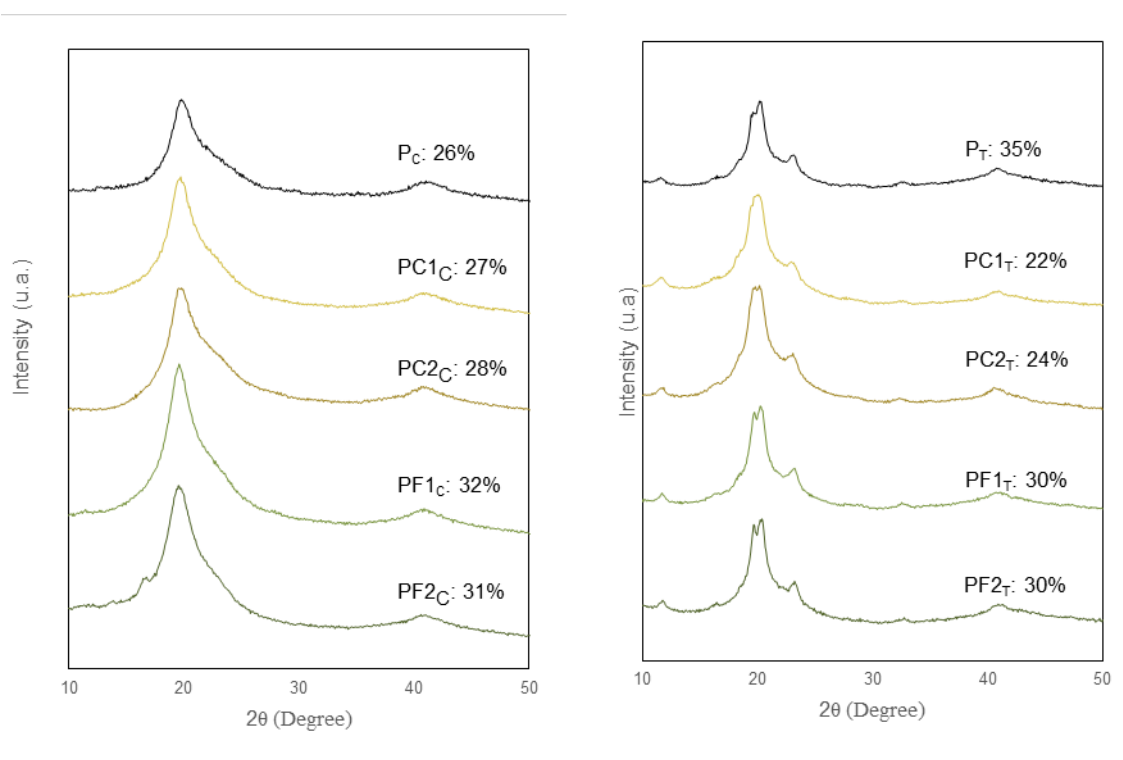
362

363 **Figure 2** shows the XRD pattern and the degree of crystallinity of the PVA  
 364 samples. As can be observed, the thermoprocessed and cast films presented  
 365 differentiated patterns, both corresponding to the characteristic XRD pattern of

366 the PVA monoclinic cell. The diffraction peaks of the thermoprocessed films were  
367 sharper, allowing for the identification of a greater number of peaks: the two main  
368 peaks (a doublet at  $2\theta = 19.5^\circ/20^\circ$  and the second at  $40.4^\circ$ ) and other peaks with  
369 less intensity at  $11.5^\circ$  and  $32.8^\circ$ , as well as a shoulder that protrudes from the  
370 main peak at  $22.8^\circ$ . In contrast, only two main peaks were observed (at  $2\theta 20^\circ$   
371 and  $40.4^\circ$ ) in the diffraction trace of the cast films. Therefore, the degree of  
372 crystallinity of the active-free PVA films obtained by thermoprocessing was  
373 greater (35%) than that obtained by casting (26%). These results are coherent  
374 with what was reported by Di Vona (2015), who stated that the processing  
375 conditions of semicrystalline polymers affect the crystal structure, the degree of  
376 crystallinity, the perfection of the crystals and the orientation of both the crystalline  
377 and amorphous phases in the films. Assender & Windle (1998) also claimed that  
378 the intensity of the peaks depends on the orientation of the hydrogen bonds, both  
379 intermolecular and intramolecular, found within a crystalline lattice. Therefore, it  
380 can be concluded that the PVA film processing method influenced the orientation  
381 of the hydrogen bonds in the crystalline unit cell, giving rise to different diffraction  
382 traces of the films and crystallinity.

383 The incorporation of phenolic acids also promoted some changes in the  
384 XRD patterns and in the degree of crystallinity of the films. Whereas this  
385 incorporation, enhanced the film crystallinity in cast films, this did not occur in  
386 thermoprocessed films. For both kinds of films, the addition of ferulic acid implied  
387 greater crystallinity than that of cinnamic acid. In thermoprocessed films, the  
388 incorporation of ferulic acid enhanced the sharpness of the diffraction peaks,  
389 which is mainly visible in the  $19.5^\circ/20^\circ$  doublet; in cast films, however, the highest  
390 concentration of ferulic acid gave rise to an additional peak at  $17.2^\circ$ , also reported  
391 as characteristic of PVA crystallisation. The p-hydroxyl group in ferulic acid could  
392 promote the interchain bonds, affecting the orientation of the hydrogen bonds  
393 inside the unit cell.

394 Therefore, thermoprocessing and the incorporation of ferulic acid promoted  
395 the crystallisation of PVA; thermal treatment in the presence of phenolic acids,  
396 however, generally implied a reduction in crystallinity, probably due to the  
397 occurrence of partial hydrolyses in the PVA chains that affect the overall chain  
398 interactions in the matrix and the plasticisation of local regions where acids could  
399 become oversaturated, as observed in FESEM images.



401

402 **Figure 2.** X-Ray diffraction spectra and percentage of crystallinity (%) of the cast  
 403 (left) and thermo-processed (right) films with and without cinnamic (C) or ferulic  
 404 (F) acid at different concentrations (1 or 2 g/100 g PVA).

405 \*(Single column/Colour should be used)

406

### 407 3.3. FTIR characterisation

408 The FTIR spectra of the active-free PVA films and those containing phenolic  
 409 acids are shown in **Annex 2**. The spectra of the films show the typical PVA bands,  
 410 without being affected by the type of processing; a broad peak at  $3270\text{ cm}^{-1}$   
 411 associated with intermolecular hydrogen bonding and hydroxyl stretching  
 412 vibration (O-H) and consecutive peaks at  $2930\text{ cm}^{-1}$  and  $2900\text{ cm}^{-1}$  due to  
 413 asymmetric and symmetric stretching vibrations. Peaks at  $1410\text{ cm}^{-1}$ ,  $1310\text{ cm}^{-1}$ ,  
 414  $1080\text{ cm}^{-1}$  and  $825\text{ cm}^{-1}$  are related to  $\text{CH}_2$  bending, carbon skeleton movement  
 415 (C-H), C-O and C-C stretching, respectively. The presence of residual acetate  
 416 groups in the polymer chain is represented by peaks at  $1737\text{ cm}^{-1}$ ,  $1706\text{ cm}^{-1}$ ,  
 417  $1365\text{ cm}^{-1}$  and  $1250\text{ cm}^{-1}$  associated with the stretching vibration bands of the  
 418 carbonyl and acetyl groups. The typical peaks of cinnamic acid (Chandran et al.,  
 419 2006; Nolasco et al., 2009) and ferulic acid (Aarabi et al., 2016) were not detected



420 in the FTIR spectra of the films containing these compounds, probably due to  
421 their low concentration in the matrices and the overlapping with the PVA peaks.  
422 Similar results were found by (Aragón-Gutiérrez et al., 2021) for EVOH films  
423 incorporating 0.25 and 1% (w/w) of ferulic acid.

424

### 425 **3.4. Tensile properties**

426 The thickness values and tensile and barrier properties of the films are  
427 shown in **Table 2**. The compression-moulded films were significantly thicker  
428 ( $p < 0.05$ ) than the cast films due to the higher surface solid density (2 and 4 g  
429 polymer per film, respectively, for cast and thermoprocessed films). The  
430 incorporation of PA reduced the film thickness in thermoprocessed samples,  
431 which may be attributed to the higher degree of flowability of the material during  
432 the thermocompression. This increase in the flowability might be due to the partial  
433 hydrolyses in PVA chains and the subsequent local plasticisation, as commented  
434 on in FESEM analyses. The tensile strength and elongation at break and stiffness  
435 of the PVA films were also influenced ( $p < 0.05$ ) by the method used to process  
436 the material. Thus, thermoprocessing generated 30% stiffer films, whereas the  
437 solvent-casting process promulgated the development of materials that were  
438 highly stretchable (E) and resistant to break (TS), and whose values almost  
439 doubled those obtained by their thermoprocessed peers. The greater stiffness of  
440 thermoprocessed films is coherent with their greater degree of crystallinity. In  
441 contrast, in the cast films, the polymer chains can unfold and orient themselves  
442 throughout the drying step, thus giving rise to a network with more oriented  
443 chains, which enhanced chain slippage during film stretching, favouring the film  
444 extensibility and, subsequently, the resistance to break. During melt blending and  
445 compression moulding, the greater viscosity of the melt limited the opportunities  
446 for the polymer chain orientation, thus promoting the development of less  
447 stretchable, more brittle matrices. So, the two film-processing methods generated  
448 materials with different molecular arrangements and degrees of crystallinity that  
449 would present different degrees of impediment in the sliding of the molecular  
450 chains, giving rise to materials of varying stiffness, elongation and resistance.  
451 Moreover, differences in the thickness and moisture contents of the films will also  
452 affect their tensile behaviour.

453 The incorporation of PA did not significantly affect ( $p>0.05$ ) the elongation at  
 454 break of the films. However, changes in the stiffness and mechanical resistance  
 455 were observed, depending on the processing method. In cast films, PA increased  
 456 stiffness and strength of the films, while the opposite behaviour was observed in  
 457 thermoprocessed films probably due to the above-mentioned effect of  
 458 hydrolyses. The established polymer-PA interactions (interchain bonds through  
 459 the chain hydroxyls and carboxyl and phenol groups) seem to enhance the load  
 460 mechanical parameters (TA, EM) in cast films, although this effect overlapped  
 461 with the potential effect of hydrolyses in thermoprocessed films, giving rise to  
 462 weakened matrices. In every case, ferulic acid promoted the film elastic modulus  
 463 and resistance to break to a greater extent, regardless of its concentration, while  
 464 cinnamic acid only provoked a significant effect when incorporated at the highest  
 465 concentration. This greater effect of ferulic could be attributed to its specific  
 466 molecular structure, with a p-hydroxyl group, that better allows for interchain  
 467 bonds and the crosslinking effect.

468

469 **Table 2.** Thickness, tensile strength (TS), elongation at break (E%) and elastic  
 470 modulus (EM), water vapour permeability (WVP) and oxygen permeability (OP)  
 471 of the PVA (P) films without and with cinnamic C and ferulic F acids (1 or 2 g/100  
 472 g PVA) obtained by casting (C) or thermo-processing (T). Mean values and  
 473 standard deviation.

Sample	Thickness ( $\mu\text{m}$ )	Tensile strength TS (MPa)	Elongation E (%)	Elastic modulus (MPa)	WVP (g mm/m <sup>2</sup> .h. kPa) ·	OP (cm <sup>3</sup> /m.h. kPa) · 10 <sup>8</sup>
P <sub>C</sub>	104 (7) <sup>a,1</sup>	47 (9) <sup>a,2</sup>	111 (9) <sup>a,2</sup>	49 (3) <sup>a,1</sup>	8.2 (0.7) <sup>b,1</sup>	13.0 (2.0) <sup>b,1</sup>
PC1 <sub>C</sub>	118 (6) <sup>b,1</sup>	47 (12) <sup>a,2</sup>	107 (8) <sup>a, 2</sup>	52 (3) <sup>ab,1</sup>	7.0 (.02) <sup>ab,1</sup>	12.0 (1.0) <sup>ab,1</sup>
PC2 <sub>C</sub>	124 (4) <sup>b,1</sup>	44 (10) <sup>a,2</sup>	107 (8) <sup>a, 2</sup>	53 (4) <sup>bc,1</sup>	8.0 (0.5) <sup>b,1</sup>	11.8 (0.4) <sup>ab,1</sup>
PF1 <sub>C</sub>	105 (8) <sup>a,1</sup>	53 (6) <sup>ab,2</sup>	111 (4) <sup>a, 2</sup>	56 (5) <sup>c,1</sup>	6.5 (0.5) <sup>ab,1</sup>	10.0 (0.9) <sup>a,1</sup>
PF2 <sub>C</sub>	103 (11) <sup>a,1</sup>	58 (6) <sup>b,2</sup>	109 (6) <sup>a, 2</sup>	57 (4) <sup>c,1</sup>	6.5 (0.2) <sup>a,1</sup>	11.3 (1.1) <sup>ab,1</sup>
P <sub>T</sub>	204 (17) <sup>b,2</sup>	25 (2) <sup>b,1</sup>	58 (7) <sup>ab,1</sup>	68 (4) <sup>c,2</sup>	11.4 (0.8) <sup>b,2</sup>	30 (4) <sup>c,2</sup>
PC1 <sub>T</sub>	189 (14) <sup>ab,2</sup>	23 (3) <sup>ab,1</sup>	55 (11) <sup>a,1</sup>	63 (2) <sup>b,2</sup>	10.5 (0.3) <sup>ab,2</sup>	24 (1) <sup>b,2</sup>
PC2 <sub>T</sub>	186 (8) <sup>a,2</sup>	20 (2) <sup>a,1</sup>	57 (4) <sup>ab,1</sup>	55 (7) <sup>a,1</sup>	9.1 (0.5) <sup>a,2</sup>	20 (2) <sup>ab,2</sup>
PF1 <sub>T</sub>	183 (12) <sup>a,2</sup>	22 (3) <sup>a,1</sup>	64 (7) <sup>ab,1</sup>	52 (2) <sup>a,1</sup>	10.2 (0.9) <sup>ab,2</sup>	17 (2) <sup>a,2</sup>
PF2 <sub>T</sub>	182 (13) <sup>a,2</sup>	23 (3) <sup>a,1</sup>	66 (5) <sup>b,1</sup>	53 (6) <sup>a,1</sup>	9.6 (1.4) <sup>a,2</sup>	17 (2) <sup>a,2</sup>

474 Different superscript letters indicate significant differences between formulations within the same processing method,  
475 while different numbers indicate significant differences between formulations with equivalent mass fractions but processed  
476 by another method ( $p < 0.05$ ).  
477 \*(2-columns)

478

### 479 **3.5. Barrier properties**

480 PVA films present good barrier capacity against oxygen due to its polar  
481 nature and the low oxygen solubility in the matrix, which limits permeability. The  
482 highly cohesive nature of the polymer matrix due to the interchain hydrogen  
483 bonds also contributes to a reduction in the oxygen permeability through the  
484 limitation of molecular mobility and diffusion. In contrast, given the high degree of  
485 polarity of the polymer, the water molecules in the matrix are highly soluble, which  
486 favours their permeation through the matrix.

487 As expected, the values of OP ( $13.10^8 \text{ cm}^3 / \text{mhKPa}$ ) and WVP ( $8.2 \text{ g mm} /$   
488  $\text{m}^2 \cdot \text{h.KPa}$ ) of the phenolic-free, glycerol-plasticised PVA cast films (Pc) were  
489 higher than those reported for non-plasticised cast films (Andrade et al., 2020b).  
490 This is coherent with the plasticising effect of glycerol in the polymer matrix which  
491 leads to weaker interactions between the chains and, therefore, to greater  
492 molecular mobility and free volume in the polymer system (Hedenqvist, 2012).

493 As can be observed in **Table 2**, thermoprocessed PVA films exhibited  
494 significantly worse barrier properties ( $p < 0.05$ ) than cast films despite their higher  
495 crystallinity values, which could be explained by the better packing of oriented  
496 chains in cast films, which inhibited molecular diffusion. Similar results were found  
497 by (Moreno et al., 2017) for starch-gelatine films obtained by both casting and by  
498 compression moulding.

499 Although the barrier properties of the films were only slightly improved by the  
500 incorporation of PA, this effect was more marked in thermoprocessed films,  
501 where WPV was reduced by up to about 10% and OP by up to 43%, when ferulic  
502 acid was incorporated. The hydrogen bonds and Lewis adducts established  
503 between PA and the PVA chains may contribute to a reduction in molecular  
504 mobility, thus reducing the rate of molecule transport throughout the matrix. In  
505 addition, the antioxidant nature of phenolic acids could also contribute to the  
506 reduction in oxygen molecule transport, improving the barrier capacity of the  
507 material. Ferulic acid was more effective than cinnamic acid at improving the

508 barrier properties of the PVA films, especially the oxygen barrier capacity. Its  
 509 molecular structure (with a p-hydroxyl group), which allows for interchain bonds,  
 510 the promotion of crystallinity and a higher antioxidant capacity than cinnamic acid  
 511 (Li et al., 2021), better contributes to an enhancement in the oxygen barrier  
 512 properties of the films than cinnamic acid. This trend has also been reported for  
 513 EVOH films with 0.25% and 0.5% of ferulic acid, which caused a decrease (25%  
 514 and 28%, respectively) in the values of the oxygen transmission rate of the films  
 515 (Aragón-Gutiérrez et al., 2021).

516

### 517 **3.6. Optical properties of the films**

518 The colour parameters (lightness ( $L^*$ ), Chroma ( $Cab^*$ ) and hue ( $hab^*$ )), and  
 519 internal transmittance pattern, used as a transparency indicator, of the different  
 520 samples are shown in **Table 3** and **Figure 3**, respectively.

521 The incorporation of phenolic acids, especially ferulic, significantly reduced  
 522 the hue values and increased the chrome, leading the film towards a more  
 523 saturated yellowish appearance, regardless of the processing method.  
 524 Nevertheless, thermoprocessed films incorporating PA were more saturated in  
 525 colour and darker than cast films, which could be derived from the partial  
 526 oxidation of acids under the thermal processing conditions. This also affected the  
 527 loss of transparency (mainly at low wavelengths: 400 and 500 nm) of the films  
 528 with ferulic acid, especially in the case of 2% ferulic, thermoprocessed films.

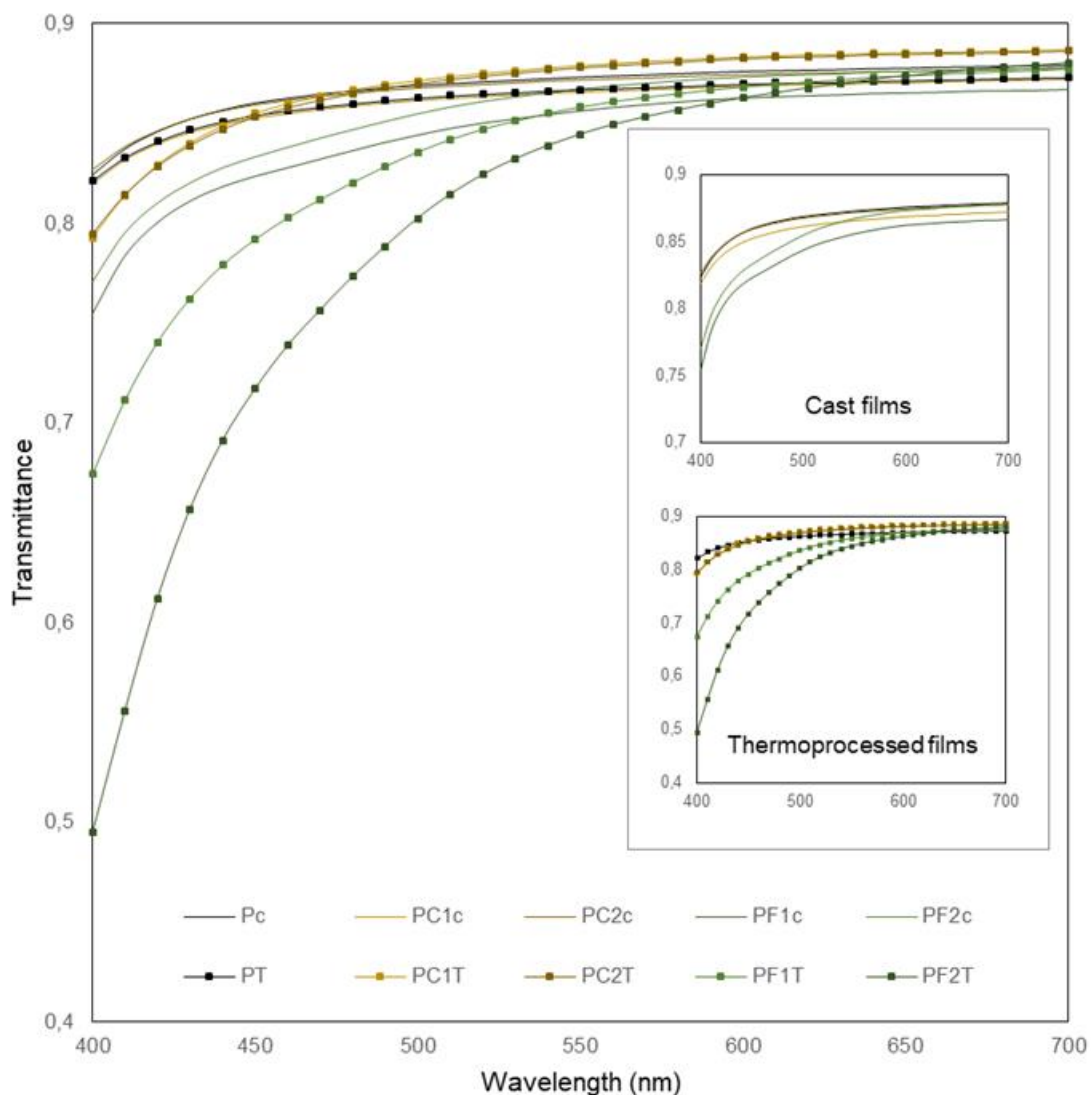
529

530 **Table 3.** Lightness ( $L^*$ ), chrome ( $Cab^*$ ), hue ( $hab^*$ ) and internal transmittance  
 531 values at 460 nm ( $T_i$ ) of the cast and thermoprocessed films of partially  
 532 hydrolysed (P) PVA films.

Sample	$L^*$	$Cab^*$	$hab^*$	$T_i$ (460 nm)
P <sub>c</sub>	90 (1) <sup>a,1</sup>	3.0 (0.1) <sup>a,1</sup>	102 (1) <sup>c,1</sup>	0.86 (0.01) <sup>c,1</sup>
PC1 <sub>c</sub>	90 (1) <sup>a,1</sup>	3.0 (0.1) <sup>a,1</sup>	102 (1) <sup>c,1</sup>	0.86 (0.01) <sup>c,1</sup>
PC2 <sub>c</sub>	90 (2) <sup>a,1</sup>	2.9 (0.1) <sup>a,1</sup>	102 (2) <sup>c,1</sup>	0.86 (0.01) <sup>c,1</sup>
PF1 <sub>c</sub>	89 (2) <sup>a,1</sup>	5.9 (0.4) <sup>b,1</sup>	99 (1) <sup>b,2</sup>	0.84 (0.01) <sup>b,2</sup>
PF2 <sub>c</sub>	89 (1) <sup>a,2</sup>	5.6 (0.6) <sup>b,1</sup>	97 (1) <sup>a,1</sup>	0.83 (0.01) <sup>a,2</sup>
P <sub>τ</sub>	90 (1) <sup>c,1</sup>	3.0 (0.1) <sup>a,1</sup>	102 (1) <sup>d,1</sup>	0.86 (0.01) <sup>c,1</sup>
PC1 <sub>τ</sub>	90 (1) <sup>c,1</sup>	4.6 (0.3) <sup>b,2</sup>	102 (1) <sup>cd,1</sup>	0.86 (0.01) <sup>c,1</sup>

PC2 <sub>T</sub>	89 (1) <sup>c,1</sup>	4.5 (0.3) <sup>b,2</sup>	101 (1) <sup>c,1</sup>	0.86 (0.01) <sup>c,1</sup>
PF1 <sub>T</sub>	88 (1) <sup>b,1</sup>	10 (1) <sup>c,2</sup>	97 (1) <sup>b,1</sup>	0.80 (0.01) <sup>b,1</sup>
PF2 <sub>T</sub>	86 (1) <sup>a,1</sup>	19 (2) <sup>d,2</sup>	96 (1) <sup>a,1</sup>	0.74 (0.01) <sup>a,1</sup>

533 Different superscript letters indicate significant differences among formulations within the same processing method, while  
534 different numbers indicate significant differences between formulations with equivalent mass fractions but processed by  
535 another method ( $p < 0.05$ ).



536  
537 **Figure 3.** Internal transmittance pattern of cast (C) and thermoprocessed (T) films  
538 of partially hydrolysed (P) PVA films with the incorporation of cinnamic (C) and  
539 ferulic (F) acid (1 or 2 g/100 g PVA).

540 \*(2-columns/Colour should be used)

541

542

### 543 3.7. Thermal behaviour

544 The first and first and second order thermal transitions, associated with  
 545 semi-crystalline materials, were analysed from the second heating scan of the  
 546 DSC analyses, as shown in **Figure 4**. The values of glass transition temperature,  
 547 melting temperature and melting enthalpy are shown in **Table 4**.

548 The thermal properties of the films were affected by the incorporation of  
 549 glycerol in the polymeric matrix, which produces significantly lower T<sub>g</sub> and T<sub>m</sub>  
 550 values than those reported for non-plasticised films, (T<sub>g</sub>: 56°C, T<sub>m</sub>: 168°C). This  
 551 effect is coherent with the plasticising effect of glycerol in the amorphous fraction  
 552 and the formation of smaller crystals, due to the interference of glycerol in the  
 553 crystallisation of the polymer (Andrade et al., 2020a). In general, the processing  
 554 method did not generate significant effects on the melting behaviour of the  
 555 materials. Nevertheless, the phenolic-free films obtained by thermo-processing  
 556 (P<sub>T</sub>) presented higher enthalpy values than films obtained by casting (P<sub>C</sub>), in line  
 557 with their higher crystallinity, as deduced from DRX spectra.

558 No remarkable changes were observed in the T<sub>g</sub>, T<sub>m</sub> or ΔH values of the  
 559 films when incorporating PA. Nevertheless, the glass transition temperature (T<sub>g</sub>)  
 560 in both cast and thermoprocessed films decreased (p<0.05) when using the  
 561 highest concentration of ferulic acid. This suggests a certain plasticising effect on  
 562 the amorphous fraction of the material, as previously reported for EVOH films  
 563 incorporating different concentrations of ferulic acid and in thermoprocessed  
 564 starch films with PA (Aragón-Gutiérrez et al., 2021). The partial hydrolysis caused  
 565 by acids under the process conditions could explain this mild plasticising effect.

566  
567

568 **Table 4.** Glass transition (T<sub>g</sub>), melting temperature (T<sub>m</sub>) and enthalpy (ΔH) of the  
 569 PVA films (P) without and with phenolic acids (1 or 2 g/100 g PVA). Mean values  
 570 and standard deviation in brackets.

Sample	Second heating scan		
	T <sub>g</sub> (°C)	T <sub>m</sub> (°C)	ΔH (J/g PVA)
P <sub>C</sub>	37 (3) <sup>b,1</sup>	154 (3) <sup>a,1</sup>	24 (1) <sup>a,1</sup>
PC1 <sub>c</sub>	37 (2) <sup>b,1</sup>	157 (1) <sup>b,1</sup>	21 (3) <sup>a,1</sup>
PC2 <sub>c</sub>	35 (1) <sup>ab,1</sup>	157 (1) <sup>ab,1</sup>	24 (3) <sup>a,1</sup>
PF1 <sub>c</sub>	38 (1) <sup>b,1</sup>	156 (1) <sup>ab,1</sup>	23 (3) <sup>a,1</sup>
PF2 <sub>c</sub>	33 (2) <sup>a,1</sup>	156 (1) <sup>ab,1</sup>	21 (1) <sup>a,1</sup>
P <sub>T</sub>	37 (1) <sup>bc,1</sup>	158 (1) <sup>a,1</sup>	27 (2) <sup>b,2</sup>

PC1 <sub>T</sub>	39 (1) <sup>cd,1</sup>	158 (1) <sup>a,1</sup>	22 (1) <sup>a,1</sup>
PC2 <sub>T</sub>	36 (1) <sup>ab,1</sup>	161 (2) <sup>a,2</sup>	25 (2) <sup>ab,1</sup>
PF1 <sub>T</sub>	39 (1) <sup>d,1</sup>	159 (1) <sup>a,2</sup>	28 (1) <sup>b,2</sup>
PF2 <sub>T</sub>	35 (1) <sup>a,1</sup>	158 (2) <sup>a,1</sup>	24 (4) <sup>ab,1</sup>

571 Different superscript letters indicate significant differences among formulations within the same processing method, while  
572 different numbers indicate significant differences between formulations with equivalent mass fractions but processed by  
573 another method ( $p < 0.05$ ).

574 \*(Single column)

575

### 576 3.7.1. Thermal degradation

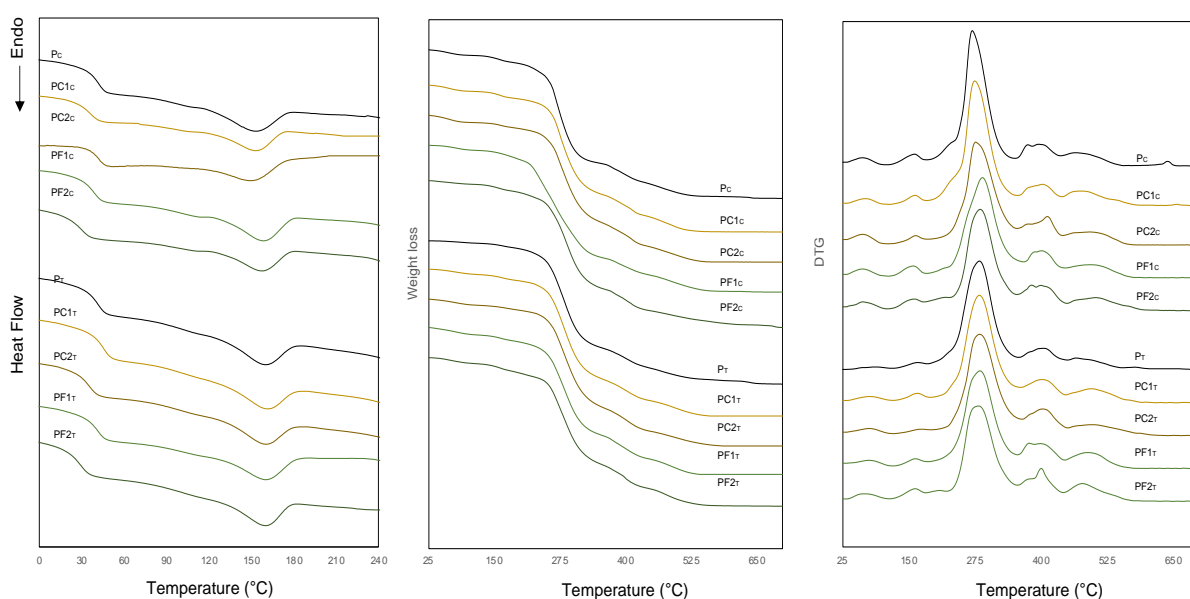
577 The thermal degradation of the samples was analysed using the curves of the  
578 thermogravimetric analysis (TGA) and its derivative (DTG), shown in **Figure 4**.  
579 The thermal degradation pattern, observed in the DTG curves, comprises  
580 multiple consecutive peaks corresponding to the degradation of the components  
581 in the polymeric matrix. The first stage corresponds to the vaporisation of the  
582 bonded water, which appeared at 62 °C and 82 °C in the casting (1.8% mass  
583 loss) and thermoprocessed (0.8% mass loss) films, respectively. The partial  
584 release of glycerol represents the second peak that occurred in the cast films (4%  
585 mass loss) at 160 °C and the thermoprocessed films (2.5% mass loss) at 167 °C.  
586 The thermo-released glycerol was less than 10% wt., concentration initially  
587 incorporated, which suggests that a fraction of the plasticiser remained closely  
588 bonded to the polymer chains due to its high affinity. The polymer degradation  
589 occurred in several stages; the first stage was associated with the detachment of  
590 side groups (hydroxyl and acetyl) from the chains, giving rise to by-products, such  
591 as acetaldehyde, acetic acid and water (Perilla, 2007). In the cast films, the main  
592 polymer degradation peak occurred at 274 °C, while in thermoprocessed films  
593 this peak moved towards higher temperatures, reaching 285 °C. This behaviour  
594 coincides with that previously reported by other authors for other matrices, such  
595 as starch-gelatine and PLA (Moreno et al., 2017; Rhim et al., 2006), indicating  
596 the early formation of degradation compounds during thermoprocessing, which  
597 may be responsible for the colour changes of these films, as previously  
598 commented on. This also points to the different chemical composition of the  
599 materials after being partially hydrolysed and/or degraded during the thermal  
600 process. Two subsequent peaks of polymer degradation were observed between  
601 350 °C and 650 °C, which were related to the degradation of low molecular weight

602 products from the polymer backbone break, or of heavier structures formed in  
603 previous stages of degradation (Holland & Hay, 2001; Perilla, 2007).

604 The thermal degradation of pure phenolic acids, between 230 °C and 280 °C  
605 (peak: 267 °C) for cinnamic acid and between 210 °C and 270 °C (peak: 250°C)  
606 for ferulic acid, was not appreciated in the thermograms of the films, due to their  
607 low mass fraction and the fact that they overlapped with the polymer degradation  
608 events.

609 The incorporation of PA only affected the thermal degradation pattern of films  
610 with ferulic acid obtained by casting, regardless of its concentration. In these  
611 films, a 10 °C increment in the temperature of the main degradation peak of PVA  
612 was observed. This indicates that this phenolic acid interfered with the thermal  
613 stability of the polymer, probably due to the interaction between its carboxyl and  
614 phenolic hydroxyl group with the hydroxyl/acetyl groups of PVA chains, giving  
615 rise to more thermally stable cross-linked films with a larger crystalline fraction,  
616 as deduced from the XRD analysis. This effect was also reported in EVOH films  
617 incorporating ferulic acid in different proportions (Aragón-Gutiérrez et al., 2021)  
618 and in PVA films with tannic acid and quercetin (Luzi et al., 2019). These acids  
619 acted as natural stabilisers against polymer degradation, in response to their  
620 characteristic chemical structure with several phenolic rings with hydroxyl groups  
621 (Luzi et al., 2019).

622



623



624 **Figure 4.** DSC (second heating scan) (left), thermogravimetric analysis (TGA)  
625 (middle) and DTGA (right) curves of the partially hydrolysed PVA films (P) without  
626 and with cinnamic (C) or ferulic (F) acid (1 or 2 g/100 g PVA).

627 \*(2-columns/Colour should be used)

628

### 629 **3.8. Antioxidant and antimicrobial capacity of the films**

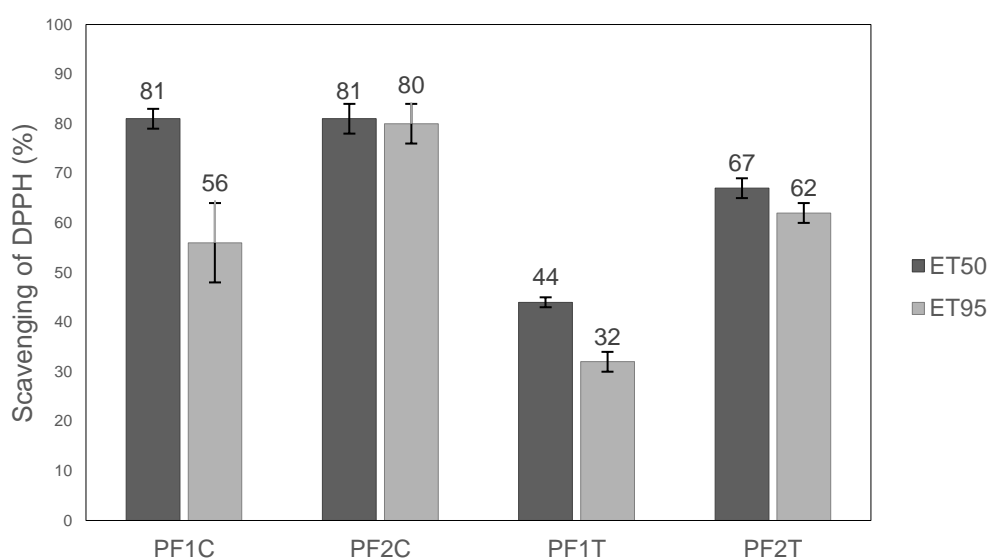
630 The antioxidant capacity of the active films was evaluated through the  
631 inhibition power of the DPPH radical of the active compounds delivered from the  
632 films into food simulants: ethanol 50% (v/v) as a simulant of O/W emulsified foods  
633 and ethanol 95% (v/v), as a simulant of lipophilic foods. No significant radical  
634 scavenging activity was observed for the films with cinnamic acid; the inhibition  
635 values ranged between 0.5 and 2%. In contrast, the inhibition capacity of ferulic  
636 acid was very high, ranging between 32% and 81% as can be observed in **Figure**  
637 **5**, depending on the film processing method and food simulant. This difference is  
638 directly related to the molecular structure, depending on the number and position  
639 of the hydroxyl groups on the benzene ring (Li et al., 2021). Thus, ferulic acid is  
640 an o-hydroxycinnamic acid with a methoxy group in the ortho position with respect  
641 to the hydroxyl in the benzene ring, a structural factor that greatly improves the  
642 hydrogen donation capacity of the phenol. The absence of a phenolic hydroxyl in  
643 the cinnamic acid structure reduces its antioxidant capacity (Li et al., 2021).  
644 Ferulic acid incorporated into EVOH films has also been proven to be highly  
645 effective at scavenging a DPPH radical (Aragón-Gutiérrez et al., 2021)

646 The inhibition values obtained for films containing ferulic acid are shown in  
647 **Figure 5**. These values will be related to the total amount of compound released  
648 from the films into the food simulant. This release depends on the solubility of the  
649 compound in the simulant and their relative chemical affinity with both the polymer  
650 matrix and the solvent, according to the corresponding partition coefficient, as  
651 well as on the relaxation of the polymer in contact with the solvent, which  
652 promotes the release rate. As can be observed in **Figure 5**, the antioxidant  
653 capacity of the films was affected by the film processing method and the food  
654 simulant. Thus, the thermoprocessed films presented a lower radical scavenging  
655 capacity than the cast films, this being about 35% and 65% for films with 1% and  
656 2% ferulic acid, respectively. This can be attributed to the partial oxidation of the

657 compound during the thermal treatment, as commented on above, which reduced  
658 the radical inhibition capacity of the films. In cast films, the inhibition of DPPH was  
659 about 80 % in every case, except in the least polar simulant (ethanol 95%) when  
660 the films contain 1% of compound, where an inhibition of only about 56% was  
661 observed, probably due to the smaller amount of ferulic acid released.

662 Finally, the greatest antioxidant capacity was found in the most polar  
663 simulant (ethanol 50%) due to the greater affinity with the PVA matrix, which  
664 favoured its swelling, thus enhancing the release of phenolic acids available to  
665 inhibit the free radicals.

666



667

668 **Figure 5.** Antioxidant activity measured through the scavenging capacity of  
669 DPPH of two food simulants (50 and 95 % ethanol in water) in contact (48 h) with  
670 PVA films containing ferulic acid (F) at 1 or 2 %, obtained by casting (C) or  
671 thermoprocessing (T).

672

673 The antimicrobial activity was only evaluated in the films with the greatest  
674 PA content (2%) by means of the disk diffusion method. The diameter of the  
675 inhibition halo of each film disk are shown in **Table 5**, for *Escherichia coli* Gram  
676 (-) and *Listeria innocua* Gram (+), as the diameter of the growth inhibition zone  
677 around the film disk. This method reflects the diffusion capacity of phenolic acids  
678 from the polymeric matrix and the sensitivity of each bacteria to compounds  
679 diffused into the agar.

680 The antibacterial activity of the films depended on the processing method,  
 681 the type of PA incorporated and the bacteria. Thus, *L. innocua*, with inhibition  
 682 halos of between 26 and 30 mm, was more sensitive to the antimicrobial effect of  
 683 the active films than *E. coli*, which exhibited smaller inhibition diameters. Ordoñez  
 684 et al., (2021) also reported this trend, when studying thermo-processed cassava  
 685 starch films incorporating C and F acids, coherent with the higher MICs of  
 686 phenolic acids of *E. Coli*.

687 As regards the film processing method, the cast films seemed to be more  
 688 effective at controlling the microbial growth than the thermoprocessed ( $p < 0.05$ );  
 689 this difference was only significant ( $p < 0.05$ ) when using C acid. So, in general,  
 690 the greatest antibacterial activity was found for cast films, regardless of the PA  
 691 incorporated. In thermoprocessed films, those with ferulic acid exhibited greater  
 692 inhibition halos ( $p < 0.05$ ) than those with cinnamic acid, despite the higher degree  
 693 of oxidation of ferulic acid in the films and the lower MIC of cinnamic acid for both  
 694 bacteria (Ordoñez et al., 2021). This suggests that the oxidated compounds of  
 695 ferulic acid could also exhibit an antimicrobial effect (Aljawish et al., 2014)

696

697 **Table 5.** Diameters of inhibition halos (mm) of bacterial growth obtained in the  
 698 agar diffusion test for film disks containing ferulic (F) or cinnamic (C) acid of cast  
 699 (C) and thermoprocessed (T) films.

Sample	Inhibition halo	
	<i>L. Innocua</i> (mm)	<i>E. coli</i> (mm)
PC2 <sub>C</sub>	29 (2) <sup>a,2</sup>	15 (3) <sup>a,2</sup>
PF2 <sub>C</sub>	30 (2) <sup>a,1</sup>	13 (2) <sup>a,1</sup>
PC2 <sub>T</sub>	26 (1) <sup>a,1</sup>	6 (2) <sup>a,1</sup>
PF2 <sub>T</sub>	29 (2) <sup>b,1</sup>	10 (2) <sup>b,1</sup>

700 Different superscript letters indicate significant differences among formulations within the same processing method, while  
 701 different numbers indicate significant differences between formulations with equivalent mass fractions but processed by  
 702 different methods ( $p < 0.05$ ).

703

704

#### 705 4. Conclusion

706 The incorporation of cinnamic and ferulic acids into the PVA films significantly  
 707 modified the physicochemical and functional properties of the films. These

708 changes were affected by the processing method (casting or thermoprocessing)  
709 and the type and concentration of phenolic acid. Thus, the addition of these active  
710 compounds improved the barrier properties of the films, especially when  
711 incorporating ferulic acid, which favours a greater degree of crosslinking in the  
712 matrix and polymer crystallinity. As concerns the processing method, cast films  
713 were more extensible and resistant to break, although thermoprocessed films  
714 were stiffer with a lower barrier capacity against water vapour and oxygen. In  
715 none of the cases was the thermal stability of the material compromised, while  
716 ferulic acid enhanced the thermal stability of the polymer in cast films. The PVA  
717 films with ferulic acid exhibited a remarkable antioxidant capacity and films with  
718 both ferulic and cinnamic acids had antilisteria properties. These results indicate  
719 that PVA films with ferulic or cinnamic acid, with modulated mechanical, barrier  
720 and antioxidant and antibacterial properties can be obtained by using casting or  
721 thermoprocessing, depending on the target application. Therefore, these are of  
722 great potential in the development of different materials for active food packaging  
723 purposes, such as coatings or films.

724

## 725 **Acknowledgement**

726 The authors also thank the services rendered by the Electron Microscopy  
727 Service of the UPV and the Nanophotonics Technology Centre of the UPV.  
728 Author Johana Andrade thanks the Departamento de Nariño-Colombia and the  
729 Fundación CEIBA for the doctoral grant.

730

731 **Funding:** This work was supported by the Ministerio de Ciencia e Innovación,  
732 Agencia Estatal de Investigación of Spain [PID2019-105207RB-I00].

733

## 734 **References**

- 735 Aarabi, A., Honarvar, M., Mizani, M., Faghihian, H., & Gerami, A. (2016).  
736 Extraction and purification of ferulic acid as an antioxidant from sugar beet  
737 pulp by alkaline hydrolysis. *Italian Journal of Food Science*, 28(3), 362–375.  
738 <https://doi.org/10.14674/1120-1770/ijfs.v143>
- 739 Aljawish, A., Chevalot, I., Jasniewski, J., Revol-Junelles, A. M., Scher, J., &  
740 Muniglia, L. (2014). Laccase-catalysed functionalisation of chitosan by ferulic  
741 acid and ethyl ferulate: Evaluation of physicochemical and biofunctional

742 properties. *Food Chemistry*, 161, 279–287.  
743 <https://doi.org/10.1016/j.foodchem.2014.03.076>

744 Andrade, J., González-Martínez, C., & Chiralt, A. (2020a). Effect of carvacrol in  
745 the properties of films based on poly (vinyl alcohol) with different molecular  
746 characteristics. *Polymer Degradation and Stability*, 179.  
747 <https://doi.org/10.1016/j.polymdegradstab.2020.109282>

748 Andrade, J., González-Martínez, C., & Chiralt, A. (2020b). Incorporation of  
749 carvacrol into poly (vinyl alcohol) films, as affected by the polymer molecular  
750 characteristics. *Polymer Degradation and Stability*.

751 Aragón-Gutiérrez, A., Rosa, E., Gallur, M., López, D., Hernández-Muñoz, P., &  
752 Gavara, R. (2021). Melt-processed bioactive evoh films incorporated with  
753 ferulic acid. *Polymers*, 13(1), 1–18. <https://doi.org/10.3390/polym13010068>

754 Assender, H. E., & Windle, A. H. (1998). Crystallinity in poly(vinyl alcohol). 1. An  
755 X-ray diffraction study of atactic PVOH. *Polymer*, 39(18), 4295–4302.  
756 [https://doi.org/10.1016/S0032-3861\(97\)10296-8](https://doi.org/10.1016/S0032-3861(97)10296-8)

757 ASTM. (2002). Standard Test Method for Tensile Properties of Thin Plastic  
758 Sheeting, ASTM D882-02. *American Society for Testing and Materials*, 14,  
759 1–10.

760 ASTM, E. (2003). *Standard Test Methods for Water Vapor Transmission of*  
761 *Shipping Containers* —. 95(Reapproved), 4–6.  
762 <https://doi.org/10.1520/D4279-95R09.2>

763 ASTM, F.-07. (2004). Standard Test Method for Determination of Oxygen Gas  
764 Transmission Rate , Permeability and Permeance at Controlled Relative  
765 Humidity Through Barrier Materials Using a Coulometric Detector 1. *Water*,  
766 98, 1–6. <https://doi.org/10.1520/F1927-07>

767 Brito, T. B. N., R.S. Lima, L., B. Santos, M. C., A. Moreira, R. F., Cameron, L. C.,  
768 C. Fai, A. E., & S.L. Ferreira, M. (2021). Antimicrobial, antioxidant, volatile  
769 and phenolic profiles of cabbage-stalk and pineapple-crown flour revealed  
770 by GC-MS and UPLC-MSE. *Food Chemistry*, 339(July 2020), 127882.  
771 <https://doi.org/10.1016/j.foodchem.2020.127882>

772 Brockhaus, S., Petersen, M., & Kersten, W. (2016). A crossroads for bioplastics:  
773 exploring product developers' challenges to move beyond petroleum-based  
774 plastics. *Journal of Cleaner Production*, 127, 84–95.  
775 <https://doi.org/10.1016/j.jclepro.2016.04.003>

- 776 Cano, A., Fortunati, E., Cháfer, M., Kenny, J. M., Chiralt, A., & González-  
777 Martínez, C. (2015). Properties and ageing behaviour of pea starch films as  
778 affected by blend with poly(vinyl alcohol). *Food Hydrocolloids*, *48*, 84–93.  
779 <https://doi.org/10.1016/j.foodhyd.2015.01.008>
- 780 Cano, A., Jiménez, A., Cháfer, M., González, C., & Chiralt, A. (2014). Effect of  
781 amylose:amylopectin ratio and rice bran addition on starch films properties.  
782 *Carbohydrate Polymers*, *111*, 543–555.  
783 <https://doi.org/10.1016/j.carbpol.2014.04.075>
- 784 Chandran, K., Nithya, R., Sankaran, K., Gopalan, A., & Ganesan, V. (2006).  
785 Synthesis and characterization of sodium alkoxides. *Bulletin of Materials*  
786 *Science*, *29*(2), 173–179. <https://doi.org/10.1007/BF02704612>
- 787 Di Vona, M. L. (2015). Encyclopedia of Membranes. *Encyclopedia of*  
788 *Membranes*. <https://doi.org/10.1007/978-3-642-40872-4>
- 789 Havstad, M. R. (2020). Biodegradable plastics. In *Plastic Waste and Recycling*  
790 (Vol. 68, Issue 9, pp. 97–129). Elsevier. [https://doi.org/10.1016/B978-0-12-](https://doi.org/10.1016/B978-0-12-817880-5.00005-0)  
791 [817880-5.00005-0](https://doi.org/10.1016/B978-0-12-817880-5.00005-0)
- 792 Hedenqvist, M. S. (2012). Barrier Packaging Materials. In *Handbook of*  
793 *Environmental Degradation of Materials: Second Edition* (Second Edi).  
794 Elsevier Inc. <https://doi.org/10.1016/B978-1-4377-3455-3.00027-4>
- 795 Hernández-García, E., Vargas, M., & Chiralt, A. (2021). Thermoprocessed  
796 starch-polyester bilayer films as affected by the addition of gellan or xanthan  
797 gum. *Food Hydrocolloids*, *113*(November 2020).  
798 <https://doi.org/10.1016/j.foodhyd.2020.106509>
- 799 Holland, B. J., & Hay, J. N. (2001). *The thermal degradation of poly ( vinyl alcohol*  
800 *)*. *42*, 6775–6783.
- 801 Hutchings, J. B. (1999). *Food color and appearance*.
- 802 Kakadellis, S., Woods, J., & Harris, Z. M. (2021). Friend or foe: Stakeholder  
803 attitudes towards biodegradable plastic packaging in food waste anaerobic  
804 digestion. *Resources, Conservation and Recycling*, *169*(January), 105529.  
805 <https://doi.org/10.1016/j.resconrec.2021.105529>
- 806 Lan, W., Zhang, R., Ahmed, S., Qin, W., & Liu, Y. (2019). Effects of various  
807 antimicrobial polyvinyl alcohol/tea polyphenol composite films on the shelf  
808 life of packaged strawberries. *LWT*, *113*, 108297.  
809 <https://doi.org/10.1016/j.lwt.2019.108297>

- 810 Li, H., Ma, Y., Gao, X., Chen, G., & Wang, Z. (2021). Probing the structure-  
811 antioxidant activity relationships of four cinnamic acids porous starch esters.  
812 *Carbohydrate Polymers*, 256(1), 117428.  
813 <https://doi.org/10.1016/j.carbpol.2020.117428>
- 814 Lim, L. T. (2015). Enzymes for food-packaging applications. In *Improving and*  
815 *Tailoring Enzymes for Food Quality and Functionality*. Elsevier Ltd.  
816 <https://doi.org/10.1016/B978-1-78242-285-3.00008-9>
- 817 Lima, M. C., Paiva de Sousa, C., Fernandez-Prada, C., Harel, J., Dubreuil, J. D.,  
818 & de Souza, E. L. (2019). A review of the current evidence of fruit phenolic  
819 compounds as potential antimicrobials against pathogenic bacteria.  
820 *Microbial Pathogenesis*, 130(December 2018), 259–270.  
821 <https://doi.org/10.1016/j.micpath.2019.03.025>
- 822 Luzi, F., Pannucci, E., Santi, L., Kenny, J. M., Torre, L., Bernini, R., & Puglia, D.  
823 (2019). Gallic acid and quercetin as intelligent and active ingredients in  
824 poly(vinyl alcohol) films for food packaging. *Polymers*, 11(12).  
825 <https://doi.org/10.3390/polym11121999>
- 826 Mathew, S., & Abraham, T. E. (2008). Characterisation of ferulic acid  
827 incorporated starch-chitosan blend films. *Food Hydrocolloids*, 22(5), 826–  
828 835. <https://doi.org/10.1016/j.foodhyd.2007.03.012>
- 829 Mileva, D., Monami, A., Cavallo, D., Alfonso, G. C., Portale, G., & Androsch, R.  
830 (2013). Crystallization of a polyamide 6/montmorillonite nanocomposite at  
831 rapid cooling. *Macromolecular Materials and Engineering*, 298(9), 938–943.  
832 <https://doi.org/10.1002/mame.201200253>
- 833 Mileva, D., Tranchida, D., & Gahleitner, M. (2018). Designing polymer  
834 crystallinity: An industrial perspective. *Polymer Crystallization*, 1(2), 1–16.  
835 <https://doi.org/10.1002/pcr2.10009>
- 836 Moreno, O., Cárdenas, J., Atarés, L., & Chiralt, A. (2017). Influence of starch  
837 oxidation on the functionality of starch-gelatin based active films.  
838 *Carbohydrate Polymers*, 178, 147–158.  
839 <https://doi.org/10.1016/j.carbpol.2017.08.128>
- 840 Nolasco, M. M., Amado, A. M., & Ribeiro-Claro, P. J. A. (2009). Effect of hydrogen  
841 bonding in the vibrational spectra of trans-cinnamic acid. *Journal of Raman*  
842 *Spectroscopy*, 40(4), 394–400. <https://doi.org/10.1002/jrs.2138>

- 843 Olszewska, M. A., Gędas, A., & Simões, M. (2020). Antimicrobial polyphenol-rich  
844 extracts: Applications and limitations in the food industry. *Food Research*  
845 *International*, 134(April), 109214.  
846 <https://doi.org/10.1016/j.foodres.2020.109214>
- 847 Ordoñez, R., Atarés, L., & Chiralt, A. (2021). Physicochemical and antimicrobial  
848 properties of cassava starch films with ferulic or cinnamic acid. *LWT*, 111242.  
849 <https://doi.org/10.1016/j.lwt.2021.111242>
- 850 Perilla, J. E. (2007). *Estudio de la degradación térmica de poli ( alcohol vinílico )*  
851 *mediante termogravimetría y termogravimetría diferencial thermogravimetry*  
852 *and differential thermogravimetry*. 27(2), 100–105.
- 853 RameshKumar, S., Shaiju, P., O'Connor, K. E., & P, R. B. (2020). Bio-based and  
854 biodegradable polymers - State-of-the-art, challenges and emerging trends.  
855 *Current Opinion in Green and Sustainable Chemistry*, 21, 75–81.  
856 <https://doi.org/10.1016/j.cogsc.2019.12.005>
- 857 Rhim, J.-W., Mohanty, A. K., Singh, S. P., & Ng, P. K. W. (2006). Effect of the  
858 processing methods on the performance of polylactide films:  
859 Thermocompression versus solvent casting. *Journal of Applied Polymer*  
860 *Science*, 101(6), 3736–3742. <https://doi.org/10.1002/app.23403>
- 861 Sapper, M., Wilcaso, P., Santamarina, M. P., Roselló, J., & Chiralt, A. (2018).  
862 Antifungal and functional properties of starch-gellan films containing thyme  
863 (*Thymus zygis*) essential oil. *Food Control*.  
864 <https://doi.org/10.1016/j.foodcont.2018.05.004>
- 865 Talón, E., Vargas, M., Chiralt, A., & González-Martínez, C. (2019). Antioxidant  
866 starch-based films with encapsulated eugenol. Application to sunflower oil  
867 preservation. *Lwt*, 113(January), 108290.  
868 <https://doi.org/10.1016/j.lwt.2019.108290>
- 869 Trabold, T., & Babbitt, Callei. W. (2018). *Sustainable Food Waste-To-energy*  
870 *Systems*. Elsevier. <https://doi.org/10.1016/C2016-0-00715-5>
- 871 Valencia-Sullca, C., Jiménez, M., Jiménez, A., Atarés, L., Vargas, M., & Chiralt,  
872 A. (2016). Influence of liposome encapsulated essential oils on properties of  
873 chitosan films. *Polymer International*, 65(8), 979–987.  
874 <https://doi.org/10.1002/pi.5143>
- 875 Vanapalli, K. R., Sharma, H. B., Ranjan, V. P., Samal, B., Bhattacharya, J.,  
876 Dubey, B. K., & Goel, S. (2021). Challenges and strategies for effective



877 plastic waste management during and post COVID-19 pandemic. *Science of*  
878 *the Total Environment*, 750, 141514.  
879 <https://doi.org/10.1016/j.scitotenv.2020.141514>

880